

Magnetoresistance through a single molecule

Stefan Schmaus,^{1,2} Alexei Bagrets,^{2,3} Yasmine Nahas,^{1,2} Toyo K. Yamada,^{1,4} Annika Bork,¹ Martin Bowen,⁵ Eric Beaupaire,⁵ Ferdinand Evers,^{3,6} and Wulf Wulfhekel^{1,2}

*¹Physikalisches Institut, Karlsruhe Institute of
Technology (KIT), 76128 Karlsruhe, Germany*

*²DFG-Center for Functional Nanostructures,
Karlsruhe Institute of Technology (KIT), 76128 Karlsruhe, Germany*

*³Institute of Nanotechnology, Karlsruhe Institute
of Technology (KIT), 76128 Karlsruhe, Germany*

*⁴Graduate School of Advanced Integration Science,
Chiba University, Chiba 263-8522, Japan*

*⁵Institut de Physique et Chimie des Matériaux de Strasbourg,
UMR 7504 UdS-CNRS, 67034 Strasbourg Cedex 2, France*

*⁶Institut für Theorie der Kondensierten Materie,
Karlsruhe Institute of Technology (KIT), D-76128 Karlsruhe, Germany*

The use of single molecules to design electronic devices is an extremely challenging and fundamentally different approach to further downsizing electronic circuits. Two-terminal molecular devices such as diodes were first predicted [1] and, more recently, measured experimentally [2]. The addition of a gate then enabled the study of molecular transistors [3–5]. In general terms, in order to increase data processing capabilities, one may not only consider the electron’s charge but also its spin [6, 7]. This concept has been pioneered in giant magnetoresistance (GMR) junctions that consist of thin metallic films [8, 9]. Spin transport across molecules, i. e. *Molecular Spintronics* remains, however, a challenging endeavor. As an important first step in this field, we have performed an experimental and theoretical study on spin transport across a molecular GMR junction consisting of two ferromagnetic electrodes bridged by a *single* hydrogen phthalocyanine (H_2Pc) molecule. We observe that even though H_2Pc in itself is nonmagnetic, incorporating it into a molecular junction can enhance the magnetoresistance by one order of magnitude to 52%.

Scanning Tunneling Microscopy (STM) has proven to be a powerful and versatile tool for studying electron transport properties of single molecules, be it by continually addressing individual molecules on a one by one level [10–13], or in an automated break junction protocol [14, 15]. In this work, we introduce spin-polarized STM (Sp-STM) to measure the magnetoresistance of single molecules, employing spin-polarized electrodes. Experiments were carried out in a home-built STM working in ultra high vacuum at 4 K [16] on individual H_2Pc molecules ($\text{C}_{32}\text{H}_{18}\text{N}_8$) sandwiched between Co-coated W tips and ferromagnetic Co nano-islands on Cu(111) single crystals.

In Fig. 1 we present the STM topography of the sample after depositing H_2Pc molecules, that identify themselves by their four aromatic isoindole (BzPy) side groups [13, 17]. We note that the Co nano-islands exhibit a spontaneous out-of-plane magnetization due to a strong surface anisotropy [18]. By using Co-coated tips (10 monolayers) with an out-of-plane magnetization, we can use the Sp-STM technique’s sensitivity to the spin-polarized density of states [19] to determine the relative orientation (parallel:P or antiparallel:AP) of the magnetization of individual islands relative to that of the tip. Fig. 1b shows the differential conductance (dI/dV) curves measured atop two islands with P and AP alignments with respect to the tip. Particularly large differences in the spectra are found at -350 meV, which

corresponds to the surface state of Co [20]. This difference allows us to detect the local magnetization direction of Co islands by recording maps of the local differential conductance at this bias voltage (see Fig. 1a). The differential tunneling magnetoresistance (differential TMR), defined as the difference in conductance divided by the smaller conductance of the tunneling junction formed by the tip and sample, is strongly energy-dependent as depicted in Fig. 1c. We note here that the differential TMR for this Co/vacuum/Co junction is only $\sim 5\%$ at low bias voltage.

To contact single molecules, we positioned the STM-tip above the aromatic side groups of a H₂Pc molecule, opened the feedback loop and decreased the tip-to-molecule distance ($\approx 1 \text{ \AA/s}$) while measuring the tunneling current. We thus obtain conductance-distance curves [10–12]. Since the observed conductances of phthalocyanine molecules are rather high [13], a small voltage (10 mV) has to be used to avoid the thermal disintegration of the molecules. We observe an exponential increase of the conductance that reflects the decreasing tunneling barrier width (see Fig. 2a). Below a certain tip-to-surface separation — typically 3-4 \AA — the conductance abruptly increases, which indicates a sudden change of the junction geometry. Similar jumps have been seen, *e. g.*, for alkanedithiol molecular wires [11]. We have recently shown that, for phthalocyanine molecules, this corresponds to a lifting of the flat H₂Pc molecule’s aromatic group as it contacts the tip [13].

The conductance after the molecular jump-to-contact depends only slightly on the distance and encompasses both the transport across the molecule G_{mol} and direct tunneling between the tip and the sample G_{tun} [11] (see Fig. 2c). This conductance G in molecular contact mode depends markedly on whether the underlying island is of P or AP type. In the particular measurement of Fig. 2a, we find $G_{\text{P}} = 0.30 G_0$ and $G_{\text{AP}} = 0.17 G_0$ measured at 10 mV bias, where $G_0 = \frac{2e^2}{h}$ is the quantum of conductance. We may eliminate a sizeable proportion of the spin-dependent direct (tip-to-island) tunneling contribution to the conductance G by subtracting the measured conductance G_{tun} before the jump from that after G_{cont} , *i. e.* $G_{\text{mol}} \approx G_{\text{cont}} - G_{\text{tun}}$.

To ensure identical tip conditions when quantitatively comparing P and AP conductances, measurements on two Co islands of P and AP type were performed in the same scan. This approach further eliminates magnetostriction of the two ferromagnetic electrodes. Each such measurement was in turn repeated several hundred times and the distribution of the P and AP conductances is depicted in Fig. 2d. The width of the conductance distribution

– which underscores the noise of the conductance measurement and a variation in contact geometries – is relatively small when compared to previous work [11]; the histogram of the measurements on nearly 800 P and AP junctions clearly reveals a difference in conductance between the P and AP junctions. Gaussian fits were used to determine the GMR from the measurement statistics. We find $G_P = (0.242 \pm 0.007) G_0$ and $G_{AP} = (0.160 \pm 0.005) G_0$. These values result in an optimistic GMR ratio of

$$\text{GMR} = \frac{G_P - G_{AP}}{G_{AP}} = (51 \pm 9)\%.$$

Surprisingly, the GMR ratio obtained at $V = 10$ mV is one order of magnitude larger than the differential TMR found for direct tunneling between the tip and the Co surface.

To understand what causes this large value of GMR, we have performed transport calculations based on density functional theory (DFT) employing the nonequilibrium Green’s function (NEGF) formalism and the TURBOMOLE package [21]; details may be found in the Supplementary Information.

To find the atomic structure of the molecular junction, we first performed a geometry optimization for H_2Pc on the Co(111) surface, represented by a cluster with 65 atoms. Our analysis suggests that H_2Pc adsorbs preferentially in the bridge position onto Co(111) (see Fig. 3a), owing to a binding energy -8.17 eV that is larger than that found in either the hollow site position (-8.06 eV) or the atop site position (-7.45 eV), consistent with earlier findings [22, 23].

We have calculated spin-polarized transport in the linear response at low bias voltage for the two junction geometries schematized in Fig. 3a,b) before (“flat”) and after (“contact”) the jump-to-contact. To establish the latter configuration, a free H_2Pc molecule has been bent along the low energy vibrational eigenmode with frequency $\omega = 6.4$ meV [13]. Within the NEGF calculations, the magnetization direction (P or AP relative to the tip) of each Co-cluster is a control parameter. We have ascertained that, in our study, the electronic structure of the Co surface is properly reproduced with, in particular, an exchange splitting of the d -states of 1.8 eV (see Supplementary Information). This leads to a magnetic moment $m(\text{Co}) \approx 1.65 \mu_B$ per surface Co atom, in agreement with previously reported calculations [24].

On a qualitative level, our transport calculations (see Fig. 3c) reproduce very well our experimental findings (see Fig. 2a). We confirm the exponentially increasing conductance in

the tunneling regime, $G_{\text{tun}}(d) \sim e^{-\beta d}$, for which the distance d between the two electrodes is still large. The slope is independent of the relative alignment of electrode magnetizations and the computational value $\beta^{\text{theo}} = 1.87 \text{ \AA}^{-1}$ (*i. e.* the work function $W^{\text{theo}} = 3.24 \text{ eV}$) is in agreement with experiment ($\beta = 1.9 \pm 0.3 \text{ \AA}$; $W = 3.2 \text{ eV}$).

Once contact between the tip and the molecule has been established, $G_{\text{cont}}(d)$ varies much more weakly with the contact distance d just as observed in the experiment. It is, however, still sensitive to the relative orientation of the magnetization of the electrodes. We find that $G_{\text{AP}}(d)$ is always much lower than $G_{\text{P}}(d)$. For a quantitative comparison with experiment, we consider the GMR^{theo} ratio at the distance d for which the ratio $r = G_{\text{tun}}/G_{\text{cont}}$ matches the value $r \approx 4$ found experimentally. We thus find that $\text{GMR}_{\text{theo}} \approx 65 \%$ and is only weakly dependent on d .

We now discuss the conduction mechanism from the substrate onto the molecule and across the molecular contact established between the tip and the aromatic group, and its impact on the large GMR measured. Pc molecules are characterized by an energetically isolated highest occupied molecular orbital (HOMO) and a nearly doubly degenerate lowest unoccupied molecular orbital (LUMO) [25]. We note that the HOMO* levels corresponding to the aromatic group hybridize only very weakly, with almost no amplitude on the bridging nitrogen (N_b)₄. By contrast, the LUMO states are located on two out of the four aromatic groups, with a strong hybridization to all N atoms forming the inner macro-cycle (see Supplementary Information). Since the N bond to Co includes states at the Fermi energy E_F [13], transport should occur via the quasi-degenerate LUMO level. We confirm this fact by examining in Fig. 3d) the transmission probability per spin direction $T_{\uparrow,\downarrow}(E)$ at the Fermi energy across a junction of P type. We find that G_{P} near E_F is indeed weighted by a peak centered slightly above E_F that underscores transmission through the LUMO level. As we discuss in the Supplementary Information, the larger density of Co minority states at E_F results, through the N-Co bond, in a larger efficiency of LUMO hybridization, and thus of LUMO broadening, in the spin \downarrow channel.

This difference in LUMO broadening for the two spin channels has a direct impact on the GMR measured across the molecular junction. Indeed, the conductance across a single level, here the LUMO, generically takes on the Breit-Wigner form [26] $G \approx \Gamma^{\text{substrate}}\Gamma^{\text{tip}}/((E_{\text{LUMO}} - E_F)^2 + (\Gamma^{\text{substrate}} + \Gamma^{\text{tip}})^2/4)$, which considers the energy separation between the LUMO and E_F , as well as the LUMO broadenings (inverse lifetimes) $\Gamma^{\text{substrate}}$

and Γ^{tip} due to hybridization to the substrate and tip, respectively. Each is in turn split into $\Gamma^{\text{min(maj)}}$ depending on the spin channel considered. Because transport is off-resonant, i.e. $|E_{\text{LUMO}} - E_{\text{F}}| \gg \Gamma^{\text{min,maj}}$, we have $G_{\text{P}} \approx (\Gamma^{\text{min}}\Gamma^{\text{min}} + \Gamma^{\text{maj}}\Gamma^{\text{maj}})/(E_{\text{LUMO}} - E_{\text{F}})^2$ while $G_{\text{AP}} \approx 2\Gamma^{\text{min}}\Gamma^{\text{maj}}/(E_{\text{LUMO}} - E_{\text{F}})^2$. Introducing the ratio $\varrho = \Gamma^{\text{maj}}/\Gamma^{\text{min}}$ we thus find

$$\text{GMR} \approx \frac{(\Gamma^{\text{min}} - \Gamma^{\text{maj}})^2}{2\Gamma^{\text{min}}\Gamma^{\text{maj}}} = \frac{(1 - \varrho)^2}{2\varrho}.$$

This simple formula implies two important rules of thumb for spin-polarized transport off-resonance across a molecule. First, the GMR is insensitive to the precise location of the resonance energy. Second, it is mainly indicative of the ratio ϱ of minority and majority molecular orbital broadenings due to hybridization. Relative to the small differential TMR ratio found between the Co substrate and tip, the larger GMR ratio measured experimentally can be explained theoretically by the above ratio ϱ . The imbalance within the two spin channels of the hybridization-induced level broadening to the molecular orbital responsible for transport promotes a high GMR across the molecule.

In conclusion, we have experimentally demonstrated a GMR of over 50% in single molecule junctions that is much larger than the value of differential TMR found without the presence of molecules in the junction. Such a high value is caused by a strong hybridization of the molecular LUMO, responsible for transport, with minority states of the two metallic electrodes. Such a selective hybridization thus leads to a spin filtering effect that could be generic to all molecular junctions.

We express our gratitude to O. Hampe, J. Kortus, K. Fink, S. Boukari, Xi Chen, M. Alouani, R. Mattana, J. van Ruitenbeek and P. Seneor for useful communications and acknowledgment support by the DFG (WU 349/3-1 and SPP1243), the Alexander von Humboldt foundation and the ANR (ANR-06-NANO-033-01).

Methods

The Cu(111) crystal was cleaned thanks to several cycles of Ar^+ sputtering and annealing. The molecules were evaporated in situ from a Knutsen cell heated to ≈ 500 K. During the deposition process we keep the sample at 270 K to reduce thermal diffusion of the deposited molecules. dI/dV curves were measured on the bare islands with the lock-in technique.

DFT-based transport calculations were carried out with a homemade code building upon the NEGF formalism and the TURBOMOLE package [21]. Our implementation enables us to perform transport simulations with free boundary conditions, which for the present case

have been extended to account for the spin-polarized electronic structure of the magnetic electrodes (for further details, see Supplementary Information). The gradient corrected approximation (GGA) DFT-energy has been amended by empirical corrections [27] to account for dispersive van der Waals interactions between the molecule and the surface.

-
- [1] Aviram, A. and Ratner, M. A. Molecular rectifiers. *Chem. Phys. Lett.* **29**(2), 277 – 283 (1974).
 - [2] Elbing, M., Ochs, R., Koentopp, M., Fischer, M., von Hänisch, C., Weigend, F., Evers, F., Weber, H. B., and Mayor, M. A single molecule diode. *Proc. Natl. Acad. Sci. USA* **102**, 8815 – 8820 (2005).
 - [3] Park, J., Pasupathy, A. N., Goldsmith, J. I., Chang, C., Yaish, Y., Petta, J. R., Rinkoski, M., Sethna, J. P., Abruna, H. D., McEuen, P. L., and Ralph, D. C. Coulomb blockade and the Kondo effect in single-atom transistors. *Nature* **417**, 722–725 (2002).
 - [4] Osorio, E. A., Bjørnholm, T., Lehn, J.-M., Ruben, M., and van der Zant, H. S. J. Single-molecule transport in three-terminal devices. *J. Phys.: Condens. Matter* **20**, 374121 (2008).
 - [5] Yu, L. H., Keane, Z. K., Ciszek, J. W., Cheng, L., Tour, J. M., Baruah, T., Pederson, M. R., and Natelson, D. Kondo resonances and anomalous gate dependence in the electrical conductivity of single-molecule transistors. *Phys. Rev. Lett.* **95**(25), 256803 (2005).
 - [6] Wolf, S. A., Awschalom, D. D., Buhrman, R. A., Daughton, J. M., von Molnar, S., Roukes, M. L., Chtchelkanova, A. Y., and Treger, D. M. Spintronics: A spin-based electronics vision for the future. *Science* **294**(5546), 1488–1495 (2001).
 - [7] Zutic, I., Fabian, J., and Sarma, S. D. Spintronics: fundamentals and applications. *Rev. Mod. Phys.* **76**, 323 (2004).
 - [8] Baibich, M. N., Broto, J. M., Fert, A., Van Dau, F. N., Petroff, F., Etienne, P., Creuzet, G., Friederich, A., and Chazelas, J. Giant magnetoresistance of (001)Fe/(001)Cr magnetic superlattices. *Phys. Rev. Lett.* **61**(21), 2472–2475 (1988).
 - [9] Binasch, G., Grünberg, P., Saurenbach, F., and Zinn, W. Enhanced magnetoresistance in layered magnetic structures with antiferromagnetic interlayer exchange. *Phys. Rev. B* **39**(7), 4828–4830 (1989).
 - [10] Joachim, C., Gimzewski, J. K., Schlittler, R. R., and Chavy, C. Electronic transparency of a single C60 molecule. *Phys. Rev. Lett.* **74**(11), 2102–2105 (1995).

- [11] Haiss, W., Wang, C., Grace, I., Batsanov, A. S., Schiffrin, D. J., Higgins, S. J., Bryce, M. R., Lambert, C. J., and Nichols, R. J. Precision control of single-molecule electrical junctions. *Nature Mat.* **5**, 995 (2006).
- [12] Néel, N., Kröger, J., Limot, L., Frederiksen, T., Brandbyge, M., and Berndt, R. Controlled contact to a C60 molecule. *Phys. Rev. Lett.* **98**(6), 065502 (2007).
- [13] Takács, A. F., Witt, F., Schmaus, S., Balashov, T., Bowen, M., Beaurepaire, E., and Wulfhekel, W. Electron transport through single phthalocyanine molecules studied using scanning tunneling microscopy. *Phys. Rev. B* **78**(23), 233404 (2008).
- [14] Venkataraman, L., Klare, J. E., Tam, I. W., Nuckolls, C., Hybertsen, M. S., and Steigerwald, M. L. Single-molecule circuits with well-defined molecular conductance. *Nano Letters* **6**, 458–462 (2006).
- [15] Li, Z., Pobelov, I., Han, B., Wandlowski, T., Błaszczuk, A., and Mayor, M. Conductance of redox-active single molecular junctions: an electrochemical approach. *Nanotechnology* **18**, 044018 (2007).
- [16] Balashov, T., Takács, A. F., Wulfhekel, W., and Kirschner, J. Magnon excitation with spin-polarized scanning tunneling microscopy. *Phys. Rev. Lett.* **97**(18), 187201 (2006).
- [17] Lippel, P. H., Wilson, R. J., Miller, M. D., Wöll, C., and Chiang, S. High-resolution imaging of copper-phthalocyanine by scanning-tunneling microscopy. *Phys. Rev. Lett.* **62**(2), 171–174 (1989).
- [18] Pietzsch, O., Kubetzka, A., Bode, M., and Wiesendanger, R. Spin-polarized scanning tunneling spectroscopy of nanoscale cobalt islands on Cu(111). *Phys. Rev. Lett.* **92**(5), 057202 (2004).
- [19] Tersoff, J. and Hamann, D. R. Theory of the scanning tunneling microscope. *Phys. Rev. B* **31**(2), 805–813 (1985).
- [20] Diekhöner, L., Schneider, M. A., Baranov, A. N., Stepanyuk, V. S., Bruno, P., and Kern, K. Surface states of cobalt nanoislands on Cu(111). *Phys. Rev. Lett.* **90**(23), 236801 (2003).
- [21] Arnold, A., Weigend, F., and Evers, F. Quantum chemistry calculations for molecules coupled to reservoirs: Formalism, implementation and application to benzene-dithiol. *J. Chem. Phys.* **126**, 174101 (2007).
- [22] Iacovita, C., Rastei, M., Heinrich, B. W., Brumme, T., Kortus, J., Limot, L., and Bucher, J. Visualizing the spin of individual cobalt-phthalocyanine molecules. *Phys. Rev. Lett.* **101**,

- 116602 (2009).
- [23] Heinrich, B. W., Iacovita, C., Brumme, T., Choi, D.-J., Limot, L., Rastei, M. V., Kortus, J., Hofer, W. A., and Bucher, J.-P. Selective bonding and apparent symmetry of single cobalt-phtahalocyanine molecules on a copper (111) surface. *Preprint* (2010).
- [24] Bagrets, A., Papanikolaou, N., and Mertig, I. Conduction eigenchannels of atomic-sized contacts: Ab initio KKR Greens function formalism. *Phys. Rev. B* **75**(23), 235448 (2007).
- [25] Rosa, A., Ricciardi, G., Baerends, E. J., and van Gisbergen S.J.A. The optical spectra of NiP, NiPz, NiTBP, and NiPc: Electronic effects of meso-tetraaza substitution and tetrabenzo annulation. *J. Phys. Chem. A* **105**, 3311 (2001).
- [26] Huisman, E. H., Gudon, C. M., van Wees, B. J., and van der Molen, S. J. Interpretation of transition voltage spectroscopy. *Nano Lett.* **9**, 3909–3913 (2009).
- [27] Grimme, S. Semiempirical GGA-type density functional constructed with a long-range dispersion correction. *J. Comp. Chem.* **27**(15), 1787–1799 (2006).

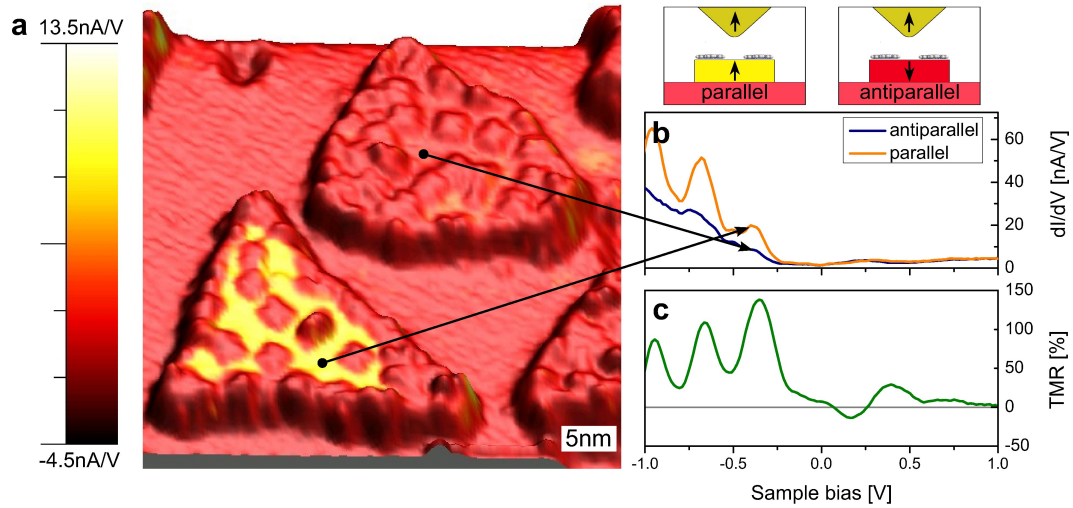


FIG. 1: a) Topographic image of H₂Pc molecules adsorbed onto two Co islands on the Cu(111) surface. The colour code displays the measured dI/dV map at -310 mV. One can distinguish between the two islands species with a magnetization parallel (P; in yellow) and antiparallel (AP; in red) with respect to the tip magnetization. b) dI/dV spectra taken on two islands of P and AP type, which clearly reveal spin-polarized states below the Fermi edge. c) Optimistic TMR ratio calculated from the dI/dV spectra. The highest value is measured at around -350 meV, and is used to distinguish between the two islands species.

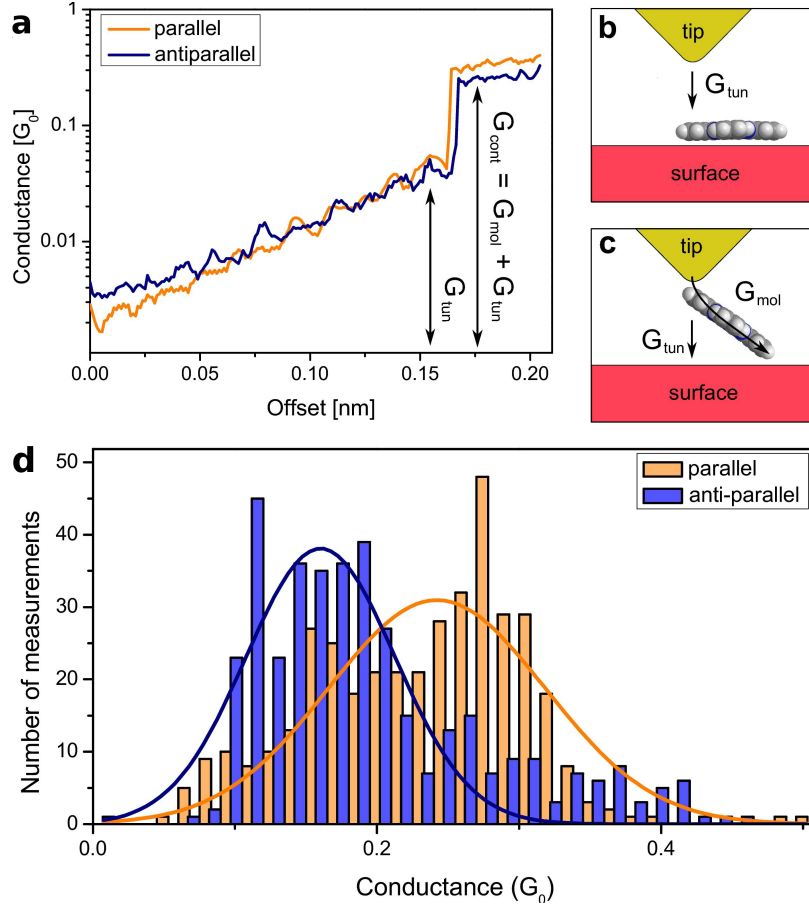


FIG. 2: a) A typical set of conductance-distance curves measured atop a H₂Pc molecule adsorbed onto P and AP magnetized islands with a constant tunneling voltage of 10 mV ($G_0 = \frac{2e^2}{h}$). As the tip approaches the molecule, the tunnel barrier width decreases, so that the conductance increases exponentially (see panel b)). Below a certain tip-to-surface separation — typically 3-4 Å — the conductance abruptly increases as the molecule jumps into contact (see panel c), and then varies only slightly upon further reducing the distance. Transport across the contacted molecule reflects both direct tunneling between the tip and the surface and conduction across the molecule (see panel c)). d) Histogram of the corrected molecular conductances (390 times parallel / 384 times antiparallel). A Gaussian fit is used to determine the statistical conductance in the P and AP configurations, and thus the GMR ratio.

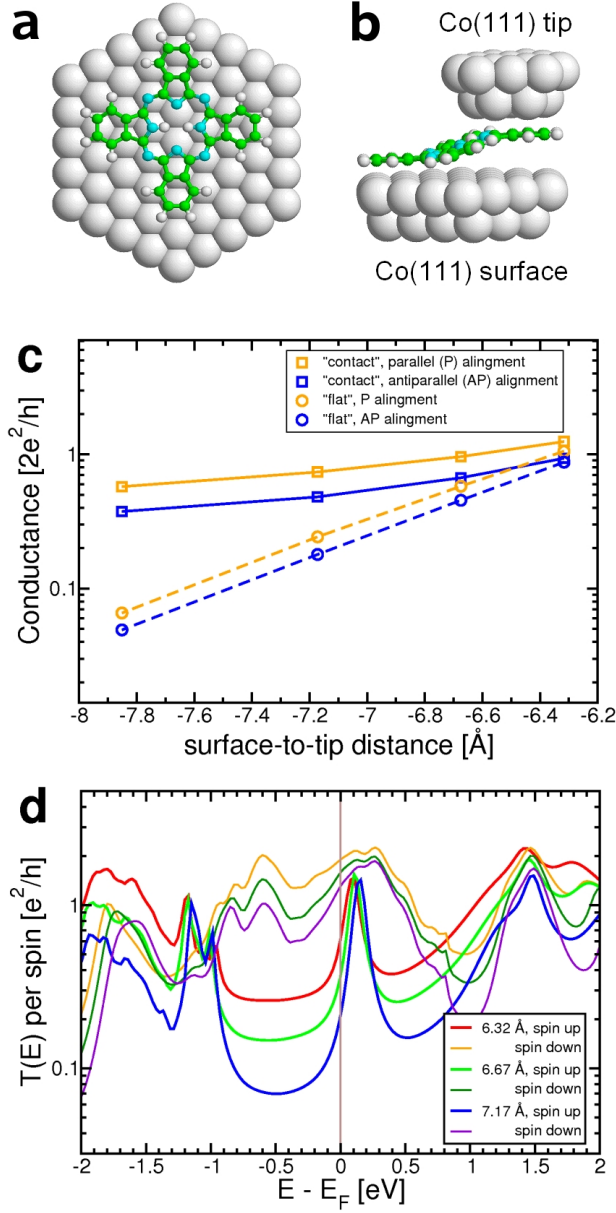


FIG. 3: a),b) Contact geometry used in the transport calculation for a H_2Pc molecule a) adsorbed on the Co-island and b) in simultaneous contact with the tip and the Co surface through a lifting of the aromatic group. Cobalt sites are in grey; hydrogen in white; carbon in green; nitrogen in cyan. c) Conductance of H_2Pc sandwiched between two P- or AP-aligned Co(111) surfaces. The upper(lower) pair of traces corresponds to the "contact"("flat") junction geometry. d) The transmission probability $T(E)$ of an electron with energy E through a molecular junction of P type for the majority (lower three traces) and minority (upper three traces) spin channels.

SUPPLEMENTARY INFORMATION:

Magnetoresistance through a single molecule

Stefan Schmaus, Alexei Bagrets, Yasmine Nahas, Toyo K. Yamada

Annika Bork, Martin Bowen, Eric Beaurepaire, Ferdinand Evers, and Wulf Wulfhekkel

1. Geometry optimization

We used the quantum chemistry package TURBOMOLE [Ref.1] to find the atomic structure of molecular junctions. We have performed standard geometry optimization for H₂Pc on Cu(111) surface, represented by a cluster with 65 atoms. (The use of Co(111)-clusters for structure optimization is impaired by the very large number of energetically almost degenerate spin multiplets.) The gradient corrected approximation (GGA [Ref.2]) DFT-energy has been amended by empirical corrections [Ref.3] to account for dispersive van der Waals interactions between the molecule and the surface. Our analysis suggests, that H₂Pc prefers the "bridge" position (see the paper, Figure 3a) with binding energy -8.17 eV, against the "hollow" site position (binding energy -8.06 eV) and "atop" site position (binding energy -7.45 eV), which is consistent with earlier findings [Refs.4,5].

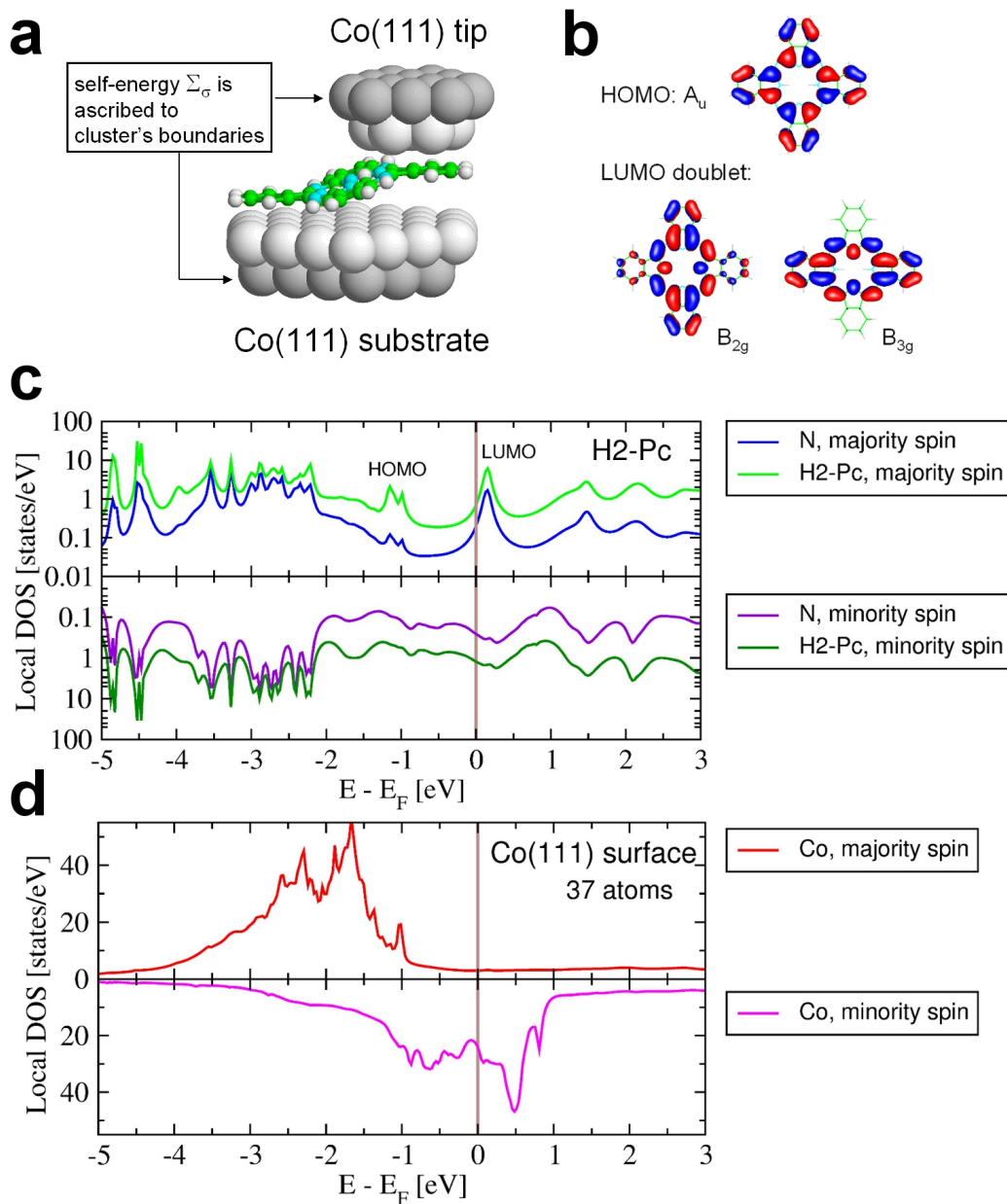
2. Electronic structure and transport calculations through H₂Pc

Density functional theory (DFT) based electronic structure and transport calculations through H₂Pc molecular junctions have been performed within the non-equilibrium Green's function (NEGF) approach as implemented in a homemade simulation code [Ref.6] interfaced to the quantum chemistry package TURBOMOLE [Ref.1]. The atomic configuration of the "extended molecule" used to simulate a bottle-neck of the molecular junction is shown in Suppl. Fig. 1a ("contact" regime): H₂Pc is bound to the two Co(111) clusters with 51 and 19 atoms, representing the Co surface and the Co STM-tip, respectively. To establish this configuration a free H₂Pc molecule has been bent along the low energy vibrational eigenmode with frequency $\omega = 6.4$ meV. A similar atomic configuration, with H₂Pc bound to the surface only, has been used for transport simulations in the tunneling regime (see the paper, Figure 3b). The generalized gradient approximation (GGA, BP86 functional [Ref.2]) and a

contracted Gaussian-type split-valence basis set with polarization functions (SVP) [Ref.7] have been employed for calculations.

First, a closed-shell (nonmagnetic) solution for the "extended molecule" comprising 2156 electrons has been found. To account for infinite reservoirs with spin-polarized electrons, the spin-dependent ($\sigma = \pm 1/2$) local self-energies, $\Sigma_{\sigma}^{\text{surface/tip}}(\mathbf{x}, \mathbf{x}') = [\lambda + \sigma \Delta_{\text{ex}} - i\gamma] \delta(\mathbf{x} - \mathbf{x}')$, have been ascribed to the outermost boundaries of the simulation cluster (dark gray atoms at Suppl. Fig. 1a). Here, a parameter $\Delta_{\text{ex}} = 1.6$ eV accounts for exchange splitting of the bulk Co d -states [Ref.8]. A freedom to choose a sign of Δ_{ex} independently for the "surface" and "STM-tip" clusters allows for two solutions: with parallel and antiparallel alignment of electrodes' magnetizations. The non-equilibrium Green's function formalism is employed to evaluate the charge- and spin-density matrices in the presence of open boundaries insuring a charge neutrality within the "extended molecule". The density matrices are given back to TURBOMOLE to find a modified set of Kohn-Sham orbitals, with a cycle to be repeated unless the self-consistent solution is reached. For the given value of the level broadening, γ ($= 1.36$ eV in present calculations), the contribution λ to the real piece of the self-energy has been defined by imposing the condition of spurious charge accumulation to be absent at the cluster's boundaries. Further details of the computational approach will be published elsewhere [Ref.9].

As an example, details of electronic structure for the molecular junction in the case of parallel alignment of magnetizations are presented in Suppl. Fig. 1c,d. The electronic states at the Co-surface are spin-polarized with exchange splitting ≈ 1.8 eV (Suppl. Fig. 1d), giving rise to an average magnetic moment $\approx 1.65\mu_B$ per a surface Co atom. Inspecting the local density of states (DOS) at H₂Pc, Suppl. Fig. 1c, we observe the majority spin resonance above the Fermi level (E_F) to be identified with the quasi-degenerate LUMO, which has a significant weight on the nitrogen atoms (cf. Suppl. Fig. 1b). In contrast, no density is seen on nitrogens for the majority spin HOMO resonance positioned ~ 1.2 eV below E_F that reflects the structure of the HOMO (Suppl. Fig. 1b). Furthermore, the minority spin H₂Pc LUMO level evolves into a broad peak due to a hybridization with the minority spin Co states, which density near E_F significantly exceeds the ones for majority spin electrons. The asymmetry in the LUMO level broadenings, $\Gamma^{\text{min}} > \Gamma^{\text{maj}}$, gives rise to a magnetoresistance effect (see text of the paper for further details).



Suppl. Fig. 1: (a) Atomic cluster, representing a bottle-neck of the H₂Pc molecular junction, used for the electronic structure and transport calculations; outermost boundaries of the Co clusters (dark gray) are subject to the absorbing boundary conditions modeled by the self-energy Σ_σ . (b) Frontier molecular orbitals of H₂Pc (D_{2h} symmetry): an A_u HOMO and a quasi-degenerate LUMO doublet, B_{2g} and B_{3g} . (c) and (d): spin-polarized local density of states at H₂Pc and Co(111) surface, respectively.

References (Supplementary Information)

- [Ref.1] TURBOMOLE V5.10 by R. Ahlrichs *et al.* (www.turbomole.com)
- [Ref.2] (a) Becke A. D. *Phys. Rev. A* **1988**, *38*, 3098; (b) Perdew J. P. *Phys. Rev. B* **1986**, *33*, 8822.
- [Ref.3] Grimme, S. *J. Comp. Chem.* **2006**, *27*, 1787–1799.
- [Ref.4] Iacovita, C.; Rastei, M.; Heinrich, B. W.; Brumme, T.; Kortus, J.; Limot, L. & Bucher, J. *Phys. Rev. Lett.* **2009**, *101*, 116602.
- [Ref.5] Heinrich, B. W.; Iacovita, C.; Brumme, T.; Choi, D.-J.; Limot, L.; Rastei, M. V.; Kortus, J.; Hofer, W. A. & Bucher, J.-P. *Selective bonding and apparent symmetry of single Cobalt-Phtahalocyanine molecules on a copper (111) surface*. Preprint, **2010**.
- [Ref.6] Arnold, A.; Evers, F. & Weigend, F. *J. Chem. Phys.* **2007**, *126*, 174101.
- [Ref.7] Schäfer, A.; Horn H. & Ahlrichs, R. *J. Chem. Phys.* **1992**, *97*, 2571.
- [Ref.8] Moruzzi, V.L.; Janak, J. F. & Williams, A. R. *Calculated Electronic Properties of Metals* (Pergamon Press, New York, 1978).
- [Ref.9] Bagrets A. **2009**, unpublished.